Vehicle Detection Based on Multi-feature Clues and Dempster-Shafer Fusion Theory

Mahdi Rezaei* and Mutsuhiro Terauchi†

*The University of Auckland, New Zealand
m.rezaei@auckland.ac.nz
† Hiroshima International University, Japan
mucha@he.hirokoku-u.ac.jp

Abstract. On-road vehicle detection and rear-end crash prevention are demanding subjects in both academia and automotive industry. The paper focuses on monocular vision-based vehicle detection under challenging lighting conditions, being still an open topic in the area of driver assistance systems. The paper proposes an effective vehicle detection method based on multiple features analysis and Dempster-Shafer-based fusion theory. We also utilize a new idea of *Adaptive Global* Haar-like (AGHaar) features as a promising method for feature classification and vehicle detection in both daylight and night conditions. Validation tests and experimental results show superior detection results for day, night, rainy, and challenging conditions compared to state-of-the-art solutions.

Keywords: Vehicle detection, Monocular vision, Collision detection, Line and corner features, Dempster-Shafer theory, Data fusion

1 Introduction

According to a recent report in 2012 by [12], rear-end crashes contribute in 33% of collisions as the highest rate among 18 types of crash studied. By maintaining early vehicle detection and warning, it is possible to provide more time for a distracted driver to take an appropriate safe maneuver to resolve driving conflicts, and consequently to decrease the possibility of rear-end crashes.

Vision-based driver assistance research addresses subjects such as vehicle detection based on analysing shadow underneath a vehicle [1, 6], stereo vision to estimate distances between *ego-vehicle* (i.e. the car the system is operating in) and obstacles [24], optical flow-based methods [2], the utilization of local binary patterns (LBP) [15, 17], or of Haar-like features [11, 13, 26].

The use of Haar and triangle features is proposed in [7]. Reported results indicate improvements compared to a standard detector using Haar features only. However, no validation tests and experiments have been considered for night conditions as well as for challenging lighting situations. Thresholding for red and white colours [16] also appears as one option to detect vehicles' taillights. However, this approach only works for night conditions, and the second weakness is that the method only works for the detection of lead vehicles which are levelled

to the ego-vehicle; a tilted vehicle (e.g. due to a road ramp, road surface at a curve, or when turning at a round about) cannot be detected by this approach.

Shadow based vehicle detection is discussed in [1, 6]. However, shadows only are unreliable indicators for the existence of a vehicle. A vehicle's shadow varies in size and position, depending on sun position.

Stereo vision and a genetic algorithm [14], or stereo vision and 3-dimensional (3D) features [24] take the advantage of depth information, represented in a disparity map, and apply inverse perspective mapping. However, the reported feature detection does not support accurate distinguishing of vehicles from other obstacles (i.e. false-positives) at night or in complicated road scenes.

A recent proposal represents a fusion technique using radar and optical flow information [5]. While the radar sensor can have multiple detections for the same vehicle, the optical flow technique can only detect overtaking vehicles with considerable velocity differences compared to the ego-vehicle.

Although we use only a monocular vision sensor for the research reported in this paper, we introduce an accurate, real-time, and effective vehicle detection algorithm to prevent imminent accidents in both day and night conditions. As a fundamental idea of this paper, we hypothesize that despite of vehicles' make, model, or colour, all vehicles have some similar features and appearances in common, including occlusion edges between vehicle and road background, different light reflectance patterns on the rear windshield compared to the body of a vehicle, a tendency towards a rectangular shape of the vehicle, and a visible shadow bar around the vehicle's rear bumper;

The paper proposes a data fusion based approach using multiple clue detection by a single camera sensor with substantial improvement in true-positive detection rate, and a lower false-positive alarm rate.

Different to other work that puts more effort into a single solution for vehicle detection, we offer a data fusion approach using a novel boosted classifier called *adaptive global Haar classification* (AGHaar) in conjunction with corner and line features to effectively detect vehicles in far and close distance as well as day and night.

The paper is organized as follows: Application of a new variant of Haar features for vehicle detection is introduced in Section 2. Section 3 discusses on line and corner feature analysis for refining initial detection results. In Section 4, a comprehensive multi-data fusion solution model is provided for robust vehicle detection based on the Dempster-Shafer theory. Section 5 provides experimental results, and Section 6 concludes.

2 Adaptive Global Haar Classifier

As an extension for standard Haar-like features, in this section we review on a recently introduced idea of *global Haar features* [21] which will be integrated in training phase of our vehicle classifier. We also improve our classifier to be *adaptive* to intensity changes to ensure robust vehicle detection at day, night, or challenging lighting conditions.

Global Haar Features. Following Viola and Jones [25], Haar features are widely used for solving various object detection problems (e.g., see [19, 26]). The value of such a Haar feature is defined by a weighted difference of image values in *white* or *black* adjacent rectangular patches, efficiently calculated by using an integral image [3].

In contrast to standard Haar features that consider adjacent black and white regions (we call them local features), here [21] as our recent work, for the first time we introduced *global Haar features*, to be used in conjunction with local features. Despite we initially used global Haar features for face detection in noisy and challenging condition, however, these features can be utilized for many other object detection purposes. Global Haar features provide global intensity information in a given sliding window, which can represent, for example, nearly uniform intensities on a road surface (i.e. when there is no other object shown in the reference window), or a nearly constant intensity of a vehicle (i.e. if a vehicle overlaps the reference window). Figure 1 represents the extraction of two global Haar-features from a given standard (local) Haar feature.

Classifier's Parameter Adaptation. Extending another recent work on eye detection under various lighting conditions [20], we try to have our vehicle classifier to be adaptive for day and night condition.

In addition to parameters that affect the training phase of a classifier (such as training feature set), there are parameters which need to be tuned during the application phase. The main parameters are: sliding window size (SWS), scale factor (SF) which specifies the rate by which SWS increases in each new iteration of the search, and the minimum number of neighbours (MNN) which is required to confirm multiple neighbour detections as a single object. Although most of research consider some fixed optimum values for these parameters, we experienced these parameters can be highly variable depending on the intensity changes of road scene. In our solution we dynamically revise and change these parameters based on road and sky intensity variation to pursue an efficient vehicle detection both in day or night conditions; see Fig. 2 for an illustration.

Instead of assigning fixed values for SWS, SF and MNN, we decide having those parameters to be time variant and adaptive, depending on the overall in-

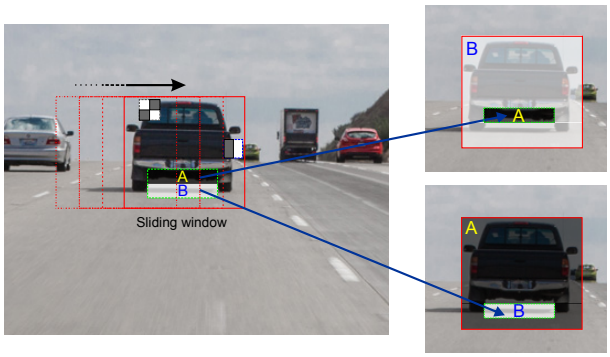

Fig. 1. *Left*: A sliding window with three local Haar features. *Right*: Extension of a given local feature into two global features.

tensity of current input frame and temporal information. For example for low light conditions, the MNN should have a smaller value than for ideal lighting conditions, because a classifier has a reduced chance of multiple object detections in dark conditions than for day light conditions. The question to be answered remains that what should be our reference for measuring the overall light intensity in an input frame?

Figure 2 illustrates pixel sampling from expected sky and road background regions, to estimate lighting conditions. We apply a 4-patch hybrid intensity averaging at expected sky and road regions, shown as S_l and S_r, and R_l and R_r; we use $w/20 \times 20$ and $20 \times h/20$ patches where w and h is width and height of the frame, respectively. Then, based on the identified lighting situation, we adaptively adjust the classifier parameters for more efficient vehicle detection.

Since a strong reflection spot, street lights, or a very dark shadow may fall in one or some of those four patches, we apply a heuristic intensity averaging including standard *mean* and *mode* (`Mo`) averaging to make sure we are measuring a balance of actual intensity in the whole scene as per below:

$$I_s(\lambda) = \frac{1}{2}\left[\left(\lambda \cdot \texttt{Mo}(S_l) + \frac{(1-\lambda)}{m}\sum_{i=1}^{m} S_l^i\right) + \left(\lambda \cdot \texttt{Mo}(S_r) + \frac{(1-\lambda)}{n}\sum_{j=1}^{n} S_r^j\right)\right]$$

where $I_s(\lambda)$ is the hybrid intensity value of the *sky* region, and m and n are the total numbers of pixels in the S_l and S_r regions.

Figure 2, on the right side, demonstrates an "acceptable" segmentation of sky and road areas. Dark and light blue segments are detected based on mean intensity measurements of S_l and S_r, with a variation of ± 10. Similarly, the green segments show the road surface based on R_l and R_r. In the shown example of a night scene (bottom, left), bright pixels occur in the S_l region; this influenced our mean-intensity measurement of the left part of the sky; consequently, dark

Fig. 2. Dynamic averaging for ground and sky region under day or night conditions.

blue segments (bottom, right) show regions around the street lights, instead of being light blue as the sky in general.

However, on the other hand, measurement in S_r supported the acceptable segmentation of the sky shown as a light-blue segment.

The *mode pixel value* (i.e. the pixel value with the highest frequency of repetition in $S_l \cup S_r$) determines which of the resulting segments (light blue or dark blue) is a better representative of the sky intensity. By assigning λ=0.66, we consider a *double importance factor* for the detected mode intensity compared to a standard mean; this consequently reduces the negative impact of any inappropriate segmentation. In other words, for the night scene shown at the bottom of Fig. 2, the final value of $I_s(\lambda)$ is automatically much closer to the intensity of light blue segments rather than to that of the dark blue segments. A similar approach is applied for road background intensity evaluation, $I_r(\lambda)$, which is shown by dark and light green segments.

As a final stage for defining the adaptive Haar-feature based detector, we experimentally adjust ten sets of optimum values for classifier parameters SWS, SF, and MNN based on values of $I_s(\lambda)$ and $I_r(\lambda)$ for the upper and lower part of the input video sequence. This parameter adaptation is then extended for the whole intensity range of 0-255 based on a cubic interpolation, as outlined in [20].

3 Line and Corner Features

The described AGHaar classifier provides us an *initial* vehicle detection. Although the proposed classifier clearly outperforms LBP and standard Haar classifiers, we still consider those detections by AGHaar as being vehicle *candidates* or *RoIs* only. In order to have more accurate results (i.e. less false-positives) we continue our evaluation by analysing line and corner features before confirming a RoI as being a vehicle.

Horizontal Edges. Instead of (e.g.) shadow analysis like [1], we take parallel horizontal edges into account as a more reliable feature for pointing to a possible existence of a vehicle in a RoI. Our hypothesis is that horizontal edge features can be perceived due to depth differences between bumper and body of a vehicle, edges around a vehicle's registration plate, or horizontal borders of windshields.

We apply the *progressive probabilistic Hough transform* (PPHT) [10] for fast and real-time detection of horizontal lines only. The PPHT was designed following the *standard Hough transform* (SHT) as introduced by Duda and Hart [4]: a line L in the xy coordinate system can be represented by polar coordinates (θ, ρ) as follows: $\rho = x \cdot cos\ \theta + y \cdot sin\ \theta$. Detected edge pixels $P_i = (x_i, y_i)$ in xy-space are transformed into curves in $\theta\rho$-space, also known as *Hough space*, or, in its discrete version, as *accumulator space*. In case of the PPHT, a voting scheme is applied to tackle with the high computational cost of SHT. While in SHT all edge pixels are mapped into the accumulator space, PPHT only votes based on a fraction of randomly selected pixels. There is one voting bin for each line candidate, and a minimum number of pixels (i.e. of votes) is considered as

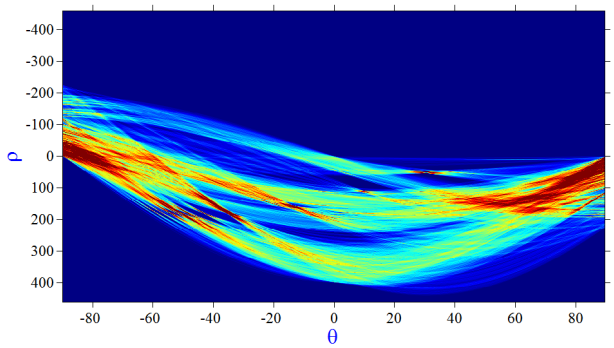

Fig. 3. Edge pixels of a sample road scene mapped into $\theta\rho$-space. The accumulator values are shown using a colour key where dark blue is for zero, red is for high values, and light blue for low positive values.

a threshold for detecting a line. For shorter lines a higher spatial density of supporting pixels is required, while for longer lines less spatial density of supporting pixels is sufficient. Overall, the PPHT ensures much faster line detection with results being about equal in accuracy with those obtained by SHT [8]. Figure 3 shows an accumulator space graph, obtained from a real world road scene. The figure illustrates that high accumulator values are close to the leftmost or rightmost borders at $-90°$ or $+90°$. This confirms for a road scene that the number of horizontal lines is considerably higher than for other slopes. In order to aim for horizontal lines $y \approx const$ we define two *ranges of interest* for θ:

$$1. \quad 90° - \tau \leq \theta \leq 90°$$
$$2. \quad -90° < \theta \leq -90° + \tau$$

Note that because ρ is considered in PPHT for positive and negative values, θ is only in the range between $-90°$ to $+90°$.

Mapping back from Hough space to Cartesian space, Figure 4-right shows detected horizontal lines for the road scene already used for Figure 3.

As illustrated, we can expect detection of one or more horizontal lines per vehicle, for any vehicle in a road scene, either for short distances or far vehicles.

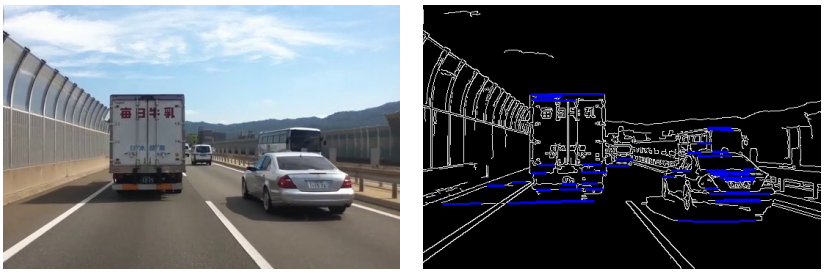

Fig. 4. Horizontal line detection by our customized PPHT.

Corner Detection. Figure 4, right, also illustrates that there might be a few more horizontal lines which do not belong to vehicles, for example due to shadows of vehicles, trees, clouds, or rectangular traffic signs (e.g. large boards). However, shaded regions or traffic signs usually have a plain or simple texture. In order to avoid false detections, we also analyse corners in the scene. Our experimental studies clearly indicate that vehicle regions have typically a higher density of corner points than road, sky, or other background regions (see Fig. 5). The visual complexity of a car's rear-view is defined by combinations of a registration plate, taillights, a bumper, and the vehicle body. This complexity defines typically significant corners for a vehicle, especially at regions down the rear windshield.

We decided for using the *Shi-Tomasi method* [23] for detecting "appropriate" corner points due to its performance in our application context. A corner is defined by larger intensity differences to adjacent pixels in comparison to non-corner image regions. In this method, an $m \times n$ subwindow W_p is considered which slides through the input image I, defined by the reference pixel $p = (x, y)$ in the upper left corner. (For example, m and n is chosen between 10 and 20.) The weighted difference between window W_p and an adjacent window of the same size, and at reference point $p + (u, v)$, is measured as follows:

$$D_p(u,v) = \sum_{i=1}^{m}\sum_{j=1}^{n} w_{ij}[I(x_i+u, y_j+v) - I(x_i, y_j)]^2 \tag{1}$$

where $0 \le u \le m/2$ and $0 \le v \le n/2$, for $x_i = x + i$ and $y_j = y + j$; w_{ij} are the used weights at window positions (i, j); they are either identical 1, or a sampled Gauss function. Using the linear terms of the Taylor expansion of those differences only, it follows that

$$\begin{aligned} D_p(u,v) &\approx \sum_{i=1}^{m}\sum_{j=1}^{n} w_{ij}[u \cdot I_x(x_i, y_j) + v \cdot I_y(x_i, y_j)]^2 \\ &= \sum_{i=1}^{m}\sum_{j=1}^{n} w_{ij}\left(u^2 I_x^2 + 2uvI_xI_y + v^2 I_y^2\right) \end{aligned} \tag{2}$$

where I_x and I_y stand for the derivatives of I in $x-$ and $y-$direction, respectively. By converting into matrix format, and not including arguments (x_i, y_j), we have that

$$D_p(u,v) \approx \begin{bmatrix} u & v \end{bmatrix} \left(\sum_{i=1}^{m}\sum_{j=1}^{n} w_{ij} \begin{bmatrix} I_x^2 & I_xI_y \\ I_xI_y & I_y^2 \end{bmatrix}\right) \begin{bmatrix} u \\ v \end{bmatrix} = \begin{bmatrix} u & v \end{bmatrix} \mathbf{M} \begin{bmatrix} u \\ v \end{bmatrix} \tag{3}$$

where $\mathbf{M}$ is short for the matrix defined in Equ. (3). Let λ_1 and λ_2 be the eigenvalues of $\mathbf{M}$, representing the differences between original and moved window, and $R = \min\{\lambda_1, \lambda_2\}$. Corner points are selected by comparing R with a given threshold; if R is greater than this threshold then the centre pixel of W_p is selected as being a corner point; see [23].

The corner points shown in Figure 5 have been detected this way. This method provides the expected results of higher corner point densities in lower

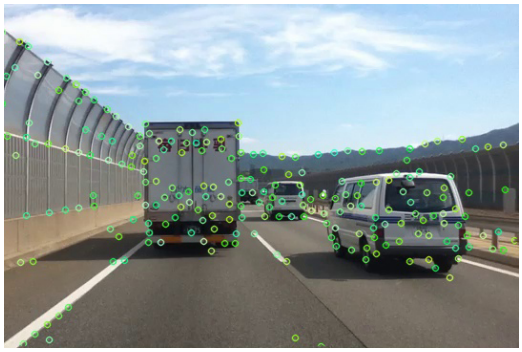

Fig. 5. Detected corner points are more dense in vehicle's back-side regions.

parts of the vehicles' rear view, especially around the registration plate, the bumper, taillights, or tires.

4 Data Fusion and Temporal Information

The AGHaar method alone is robust enough in a majority of road scenarios but not for challenging lighting conditions. However, in order to ensure an even more reliable technique we apply data fusion for all the available information clues.

As possible approaches for data fusion, we considered the Bayesian or the Dempster-Shafer [22] framework. The Bayesian method interprets weights of input entities as probabilities. The Dempster-Shafer theory (also called *theory of belief*, or *D-S theory* for short) assigns "masses" based on human expertise which only approximate the concept of probabilities. Since the Bayesian approach is based on "pure" statistical analysis, you also need to be "pure" (i.e. very accurate) on providing all statistical data for each source of information. This, consequently, comes with the requirement of a comprehensive initial database analysis among a wide range of recorded videos from different roads scenes. If not doing so, resulting inaccurate weight assignments can cause completely wrong outcomes of data fusion [9].

The D-S theory is well-known for its effectiveness to express uncertain judgments of experts by serving as an alternative method of modelling evidence and uncertainty compared to the Bayesian probabilistic approach. The D-S theory is based on two ideas: *(1)* Define a degree of belief to identify "subjective probabilities" for a related question, and *(2)* Dempster's rule to combine degrees of belief from independent items of evidence.

Using D-S theory for data fusion for vehicle detection, we not only consider two categories of "vehicle" and "no-vehicle" but also we assign a degree of belief for an "unknown" status. Considering a mass for the "unknown" status we are adding a safety margin to avoid potential wrong decisions. This automatically takes us to more rational decisions based on a combination of information consensus and human expertise; whereas in the Bayesian technique, we only have two probability values (for "existing" or "not existing"), but not a combination of both.

Table 1. Mass assignments for three sources of information.

Status	Source 1 (m_1) *AGHaar*	Source 2 (m_2) *Corner features*	Source 3 (m_3) *Horizontal lines*
T	75%	55%*	65%*
NT	15%	15%	20%
U	10%	20%	15%
Total	100%	100%	100%

* Maximum mass value if features match with threshold τ.

In the considered context we experienced that a D-S theory-based fusion approach leads to more acceptable results, especially if we have incompleteness of information and a situation where the accuracy of each information source cannot be assured individually.

Let $\mathcal{C} = \{T, NT\}$ be the set representing the state of vehicle detection from each of the three available information sources described in Sections 2 and 3 (i.e. AGHaar, corner features, and horizontal lines) where T represents that target (vehicle) is detected, and NT stands for non-target. Each element in the power set $2^{\mathcal{C}} = \{\ \emptyset,\ \{T\},\ \{NT\},\ \{T, NT\}\ \}$ is considered to be a proposition concerning the actual state of the vehicle detection system.

Based on the theory of evidence, a mass m_i is assigned for each element in $2^{\mathcal{C}}$, where $1 \leq i \leq 3$ stands for the considered information source. Value $i = 1$ is for AGHaar, $i = 2$ for corner features, and $i = 3$ for horizontal lines. Those three functions m_i are also called *basic belief assignments for information sources* 1, 2, and 3, satisfying $m_i : 2^{\Theta} \rightarrow [0, 1]$ with the two properties

$$m_i(\emptyset) = 0 \quad \text{and} \qquad \sum_{A \in 2^{\Theta}} m_i(A) = 1$$

The mass $m_i(A)$ represents the ratio of all relative and available evidences that support the validity of state A from the i^{th} information source.

For example, considering AGHaar as our main sources of vehicle detection, we consider $m_1(T) = 0.75$, $m_1(NT) = 0.15$, and $m_1(U) = 0.1$ which means that we have a belief into the true detection rate by AGHaar in 75% of all cases, we also have a 15% belief for false detections, and have no opinion in 10% of the cases (unknown assignment) due to lack of knowledge or incompleteness of analysis. Table 1 summarizes the masses defined for the three information sources.

Depending on size and distance of rectangular regions selected by AGHaar as vehicle candidates, we expect a number of corners and horizontal lines that fall into the lower part of the RoI if the candidate is actually a true positive (a vehicle).

The closer to the chosen threshold τ (as defined above) the more the possibility of being confirmed as a vehicle. In other words, if the numbers of detected corners and horizontal lines are less than the defined threshold then we decrease our level of belief by appropriately decreasing the default masses of m_2(T) and

m_3(T), and, on the other hand, by increasing $m_2(NT)$ and $m_3(NT)$ to reject the false candidates in the fusion process. However, m_2(U) and m_3(U) remain unchanged.

Also, in order to prevent incorrect updates of m_2 and m_3 due to noise, we apply weighted averaging on the masses by considering the masses allocated for n (e.g., $n = 5$) past frames to utilize temporal information as well:

$$\overline{m}_i = \frac{\sum_{t=1}^{n} \delta_t \; m_i}{\sum_{t=1}^{n} \delta_t} \tag{4}$$

In case $n = 5$ we choose, for example, $\delta_5 = 0.5$ and $\delta_1 \ldots \delta_4$ are set to be 0.2.

Considering 30 frame processing per second, in our 3.2 GHz Corei7 platform, the masses in the past few frames should remain almost close to the actual updated values as per previous step, or just having a 'smooth' change. If a sudden change happens in the current frame due to considerable noise (e.g. intense light) then the weighted averaging contributes to the masses from temporal information to maintain a moderated mass for the current frame.

Considering the masses m_i as being the confidence in each element of $2^{\mathcal{C}}$, we measure the combined confidence value $m_{1,2,3}(Z)$ by fusing information from Sources 1 to 3 following Dempster's rule of combination:

$$m_{1,2,3}(Z) = (m_1 \oplus m_2 \oplus m_3)(Z) = \frac{\sum\limits_{A \cap B \cap C = Z} m_1(A) \cdot m_2(B) \cdot m_3(C)}{1 - \sum\limits_{A \cap B \cap C = \emptyset} m_1(A) \cdot m_2(B) \cdot m_3(C)} \tag{5}$$

where $\oplus$ denotes the orthogonal sum which is defined by summing the mass product over all elements in the numerator part whose intersections are $A \cap B \cap C = Z$, and the denominator applies normalization in the range of $[0, 1]$.

5 Experimental Results

In order to validate the proposed method we used the iROADS dataset [18] that includes a diverse set of road scenes, recorded in day, night, under various weather and lighting conditions. Figures 6 and 7 show sample results and *receiver operating characteristic* (ROC) curves for situation *day*. LBP based classification shows the lowest detection rate and the highest rate of false positives. While AGHaar alone performs better than LBP and Standard Haar detector, the D-S fusion-based method outperforms the best results with a smaller rate of false alarms. Figures 8 provide samples of results for rainy night conditions. In contrast to results for situation *day*, for situation *night* the AGHaar method did not perform visibly better than standard Haar. This is mainly due to reflections of street lights on rain droplets (see Fig. 8, top) which lead to false alarms. However, the D-S fusion method shows still a high true detection rate, similar to situations *day*, with only a minor increase in false alarms (raised from 10 to 19) which is a very small portion considering the total number of true detections in our test database.

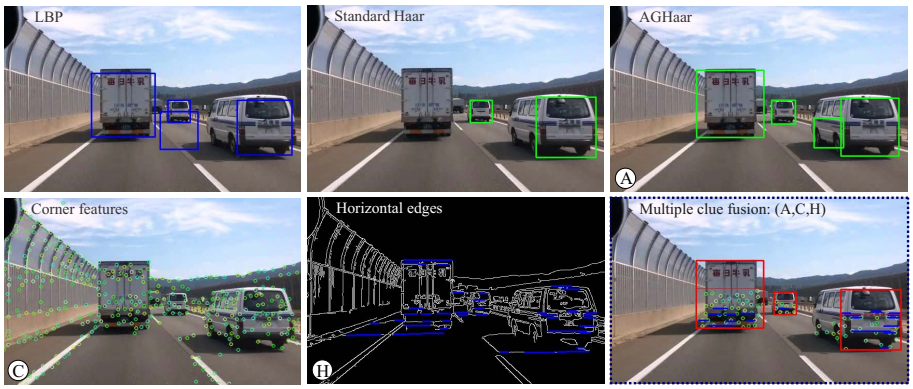

Fig. 6. Vehicle detection for situation *day* light. *Top row*: Left to right: LBP based detections, standard Haar-like classification, improved detections based on AGHaar method. *Bottom row*: Left to right, Detected corner features in road scene. Horizontal edges detected, Fusion-based detection based on AGHaar RoI, corner and edges clues.

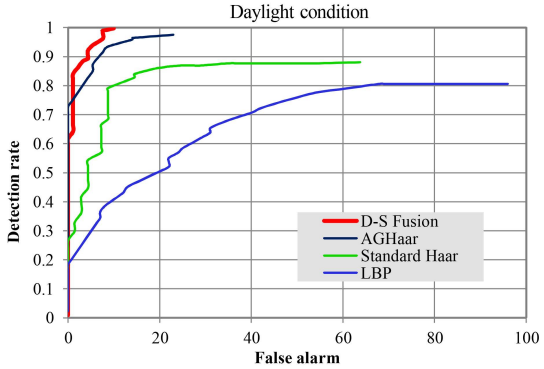

Fig. 7. Performance evaluation for situation *day*.

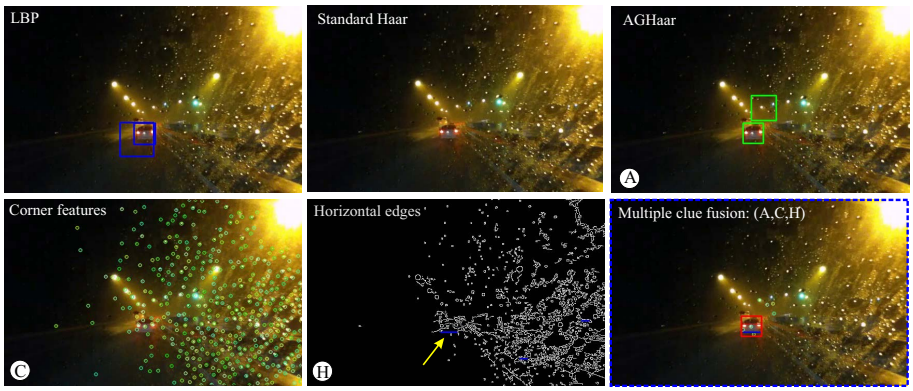

Fig. 8. Vehicle detection in situation *night*. Description of images as in Fig. 6.

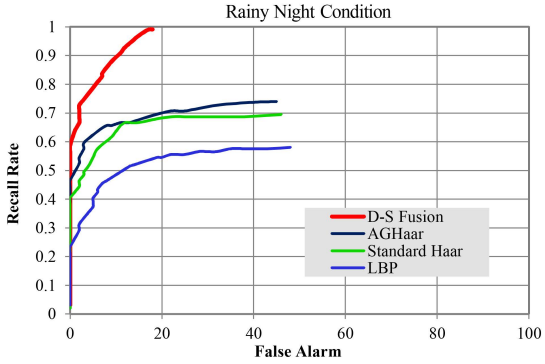

Fig. 9. Performance evaluation for situation *night*.

6 Concluding Remarks

The paper outlined an efficient proposal for monocular vehicle detection using only camera data recorded in a driving vehicle. Experimental results proved a superior performance based on the AGHaar classifier and multiple feature clue fusion, compared to the well known methods of LBP or standard Haar-like classifier.

Low computational cost of the implemented D-S fusion technique allowed us to keep maintaining real-time processing while taking the advantages of Multi-source data, extracted from only a single camera.

Validation tests on the comprehensive iROADS dataset also confirmed the robustness of the method across diverse lighting and weather conditions.

Acknowledgment: The authors thank professor Reinhard Klette for discussions and comments on the paper.

References

1. Ali, A., Afghani. S.: Shadow based on-road vehicle detection and verification using Haar wavelet packet transform. In Proc. IEEE Int. Conf. Information Communication Technologies, pp. 346–350 (2005)
2. Choi, J.: Realtime on-road vehicle detection with optical flows and Haar-like feature detectors. Technical Report, CS Department, University of Illinois at Urbana-Champaign, (2006)
3. Crow, F.: Summed-area tables for texture mapping. Computer Graphics 18, 207–212 (1984)
4. Duda, R. O., Hart P. E.: Use of the Hough transformation to detect lines and curves in pictures. Communication ACM, 15, 11–15 (1972)
5. Garcia, F., Cerri. P., Broggi, A. Escalera, A. Armingo, J. M.: Data fusion for overtaking vehicle detection based on radar and optical flow. In Proc. IEEE Intelligent Vehicles Symposium, pp. 494–499 (2012)
6. Han, S., Han, Y. Hahn, H.: Vehicle detection method using Haar-like feature on real time system. In Proc. World Academy of Science, Engineering and Technology, pp. 455–459 (2009)

7. Haselhoff, A., Kummert, A.: A vehicle detection system based on Haar and triangle features. In Proc. IEEE Intelligent Vehicles Symposium, pp. 261–266 (2009)
8. Kiryati N., Eldar Y., Bruckstein A.M.: A probabilistic Hough transform. Pattern Recognition, 24, 303–316 (1991)
9. Koks D., Challa S.: An introduction to Bayesian and Dempster-Shafer data fusion. Technical report DSTO-TR-1436, DSTO Systems Sciences Laboratory, (2005)
10. Matas, J., Galambos, C., Kittler, J.V.: Robust detection of lines using the progressive probabilistic Hough transform. Computer Vision Image Understanding, 78, 119–137 (2000)
11. Moutarde, F., Stanciulescu, B. Breheret, A.: Real-time visual detection of vehicles and pedestrians with new efficient AdaBoost features. In Proc. Workshop Planning Perception Navigation Intelligent Vehicles, (2008)
12. National Highway Traffic Safety Administration.: Traffic safety facts, U.S. Department of Transportation (2012)
13. Nguyen, T. T., Grabner, H., Bischof, H., Gruber, B.: On-line boosting for car detection from aerial images. In Proc. IEEE Int. Conf. Research Innovation Vision Future, pp. 87–95 (2007)
14. Nguyen, V. D., Nguyen, T. T., Nguyen, D. D., Jeon, J. W.: Toward real-time vehicle detection using stereo vision and an evolutionary algorithm. In Proc. Vehicular Technology Conf., pp. 1–5 (2012)
15. Ojala T., Pietikäinen, Mäenpää, T.: Multiresolution grey-scale and rotation invariant texture classification with local binary patterns. IEEE Trans. Pattern Analysis Machine Intelligence, 24, 971–987 (2002)
16. O'Malley, R., Jones, E., Glavin, M.: Rear-lamp vehicle detection and tracking in low-exposure colour video for night conditions. IEEE Trans. Intelligent Transportation Systems, 11, 453–462 (2010)
17. Qian, Z., Shi, H., Yang, J.: Video vehicle detection based on local features. Advanced Materials Research, 186, 56–60 (2011)
18. Rezaei M., Terauchi, M.: iROADS dataset (Intercity Roads and Adverse Driving Scenarios). Available in enpeda image sequence analysis test site – EISATS, Set 10. `www.mi.auckland.ac.nz/EISATS` (2013)
19. Rezaei, M., Klette, R.: Simultaneous analysis of driver behaviour and road condition for driver distraction detection. Int. J. Image Data Fusion, 2, 217–236 (2011)
20. Rezaei, M., Klette, R.: Adaptive Haar-like classifier for eye status detection under non-ideal lighting conditions. In Proc. Image Vision Computing New Zealand, pp. 521–526 (2012)
21. Rezaei, M., Ziaei Nafchi, H., Morales, S.: Global Haar-like Features: A New Extension of Classic Haar Features for Efficient Face Detection in Noisy Images. 6th Pacific-Rim Symposium on Image and Video Technology, (2013)
22. Shafer, G.: A Mathematical Theory of Evidence. Princeton University Press, (1976)
23. Shi, J., Tomasi, C.: Good features to track. In Proc. Computer Vision Pattern Recognition, pp. 593–600 (1994)
24. Toulminet, G., Bertozzi, M., Mousset, S., Bensrhair, A., Broggi, A.: Vehicle detection by means of stereo vision-based obstacles features extraction and monocular pattern analysis. IEEE Trans. Image Processing, 15, 2364–2375 (2006)
25. Viola, P., Jones, M.: Rapid object detection using a boosted cascade of simple features. In Proc. Computer Vision Pattern Recognition, pp. 511–518 (2001)
26. Wen, X., Yuan, H., Yang, C., Song, C., Duan, B., Zhao, H.: Improved Haar wavelet feature extraction approaches for vehicle detection. In Proc. IEEE Intelligent Transportation Systems Conf, pp. 1050–1053 (2007)